SPACE BASED OPTICAL OBSERVATION OF SMALL DEBRIS OBJECTS

H. Krag[(1)], M. Kahl[(1)], J. Bendisch[(1)], H. Klinkrad[(2)], T. Schildknecht[(3)]

[(1)]Institut für Luft- und Raumfahrtsysteme (aerospace systems), TU Braunschweig, Hans-Sommer-Str. 5, D-38106 Braunschweig, Germany, Email: h.krag@tu-bs.de
[(2)]European Space Operations Centre (ESA/ESOC), Robert-Bosch-Str. 5, D-64293 Darmstadt, Germany, Email: heiner.klinkrad@esa.int
[(3)]Astronomical Institute, University of Berne, Sidlerstrasse 5, CH-3012 Berne, Switzerland, Email: schild@aiub.unibe.ch

ABSTRACT

Ground based radars and telescopes are the only means to provide information about the hazardous uncatalogued space debris objects. But due to their limited sensitivity and observational constraints they leave an observational gap of mm- and cm-sized objects in higher altitudes. However, information about smaller objects in all regions is required for the validation of debris models. Passive space based telescopes are the most cost effective means to provide the required data. Results from simulation runs with the PROOF tool show the impact of sensor orbit and viewing geometry on the kind and number of objects crossing the FOV cone. The influence of the design and operation parameters of the telescope on the detected objects is discussed. Observational aspects for three possible sensor orbits (SSO, GTO and GEO) are analysed. It is shown that space based telescopes employed in a low-cost mission can fill the observational gap to a high degree.

1. INTRODUCTION

Since the awareness of the hazard resulting from the numerous space debris objects, high effort is spend on assessing the number and distribution of the objects. With the knowledge of qualitative and quantitative object fluxes, this hazard can be considered within the planning of missions. While larger objects can be regularly tracked by the USSPACECOM facilities and thus are catalogued with all their relevant parameters, information on smaller objects is rare. Here, the objects between 1mm and 10cm in LEO and 1cm and 1m in GEO are of special interest: These objects are critical as they are too small for an orbit determination by tracking facilities but still large enough to cause serious damage in the case of collisions. For these objects, usually only a few orbit parameters can be determined by measurements. Models, on the other hand, provide the full range of parameters but are incomplete and inaccurate as they are based on generalised approaches. A reliable description of the space debris environment in the critical diameter regime can thus only be obtained when models are adjusted according to and validated with measurement results. This underlines the urgent need for more data concerning the critical diameters.

In situ measurements, due to the low probability for impacts of larger objects, are restricted to the detection of objects < 1mm and thus not of interest in connection with the validation in the critical diameter regime. Currently, only optical telescopes and radar systems are capable of providing data in this area. Here, statistical information is obtained during observation campaigns like beampark experiments. However, optical and radar sensors are subjected to their limited sensitivity and geometric constraints, such as the latitude of the site that might exclude the observation of lower inclination bands. For the telescope the Sun and Moon positions are relevant and atmospheric effects add a high share of disturbing contributions to the incoming signal.

An orbital sensor will operate independently from several of these constraints. In addition, with a proper choice of the orbit, the sensor can be put directly into the region of interest. Several sensor configurations are possible for such a mission: Active instruments like radars and lidars and passive optical telescopes (see [4]). Active instruments are independent from observational conditions but the minimum detectable diameter is a function of $1/r^4$ (with r = range) and the demands for the power supply are comparably high.

This paper will concentrate on the analysis of passive optical instruments in orbit. At present, they constitute the most practical and cost effective means for this purpose. The application of CCD cameras ensures a convenient sensitivity and allows the reduction of the photometric signal in terms of object size and velocity. For the estimation of the trajectory, triangulation techniques can be applied. The instrument could be installed on a minisatellite for pick-a-back flight or, if small enough, as an experiment on a larger commercial or scientific payload. In this context, the sensor orbits analysed here, are chosen according to those of the larger class payloads.

Proceedings of the 3rd European Conference on Space Debris, ESOC, Darmstadt, Germany, 19 - 21 March 2001
(ESA SP-473, August 2001)

2. SIMULATING SPACE BASED TELESCOPES

2.1 The ESA PROOF'99 tool

The results presented here are based on deterministic simulations of the defined scenarios. In this simulation a very realistic description of the environment and observing conditions is possible. The tool enabling this is the ESA PROOF (Program for Radar and Optical Observation Forecasting) software (see [1]). This software is capable of simulating any ground- or space based optical or radar sensor for debris measurements. The main purpose of PROOF is the validation of debris models by the comparison with measurement results. The debris model is used for simulations of measurement campaigns. The comparison of the simulation results with the data obtained during the real campaigns allows deductions on the deficiencies in the space debris model. These capabilities and characteristics of PROOF also qualify it for the planning of observation campaigns based on an accurate debris model. Here, the tool is applied with the MASTER'99 model, which covers object diameters larger than 1µm in altitudes from LEO to GEO.

In the simulation process a two step filter is applied on the population: The first filter selects objects that geometrically cross the FOV cone of the sensor (crossing objects). No sensitivity is reflected yet, sensor and debris motion are considered. Basic pass characteristics like range, range-rate, and angular velocity are recorded and transferred to the second filter stage. The second filter processes the preselected set with respect to the performance of the optical instrument (detected objects). The time dependent phase angle of the objects and the pixel dwell times are determined, resulting in a signal share per pixel. Optical parameters like the aperture, point spread function, integration time and system noise are considered for that. The different background signal terms for the space based scenario are: Background stars, galaxies, planets and zodiacal light. The stars are processed semi-deterministically, using statistics on number and magnitude and deterministic imaging and trace generation on the matrix. The Earth's shadow and passes of Moon, Earth and Sun through the sensor's FOV are reflected as well.

The subset of the MASTER'99 population used here comprises objects larger than 1mm subdivided in 3 source terms. Fragments and large objects that are modelled as randomly tumbling plates, NaK reactor coolant droplets (modelled as spheres) and Solid Rocket Motor slag (modelled as randomly tumbling plates). The albedo distribution is assumed to follow a log-normal probability density with a mean of 0.1 and a standard deviation of 0.05 for all objects. In contrast to other parameter studies carried out before ([2], [3] and [4]), due to the deterministic approach, the character of this analysis is very close to that of real measurements.

2.2 Instrument design considerations

The space based sensor discussed here will have to face both, technical and cost constraints. The aperture of the telescope which has a major impact on the minimum detectable diameter is at the same time the main driver for the costs as its diameter determines the size of the whole instrument. Here an instrument aperture of 10cm is assumed to be a justifiable compromise between performance and costs.

Fig. 1 shows the signal to noise ratio (SNR) in dependence of the object diameter and range for an examplary sensor on a Sun Synchronous Orbit (SSO). The curves represent the trend obtained from PROOF data. The impact of the different angular velocities of the objects can be estimated from the spreading of the points for each diameter.

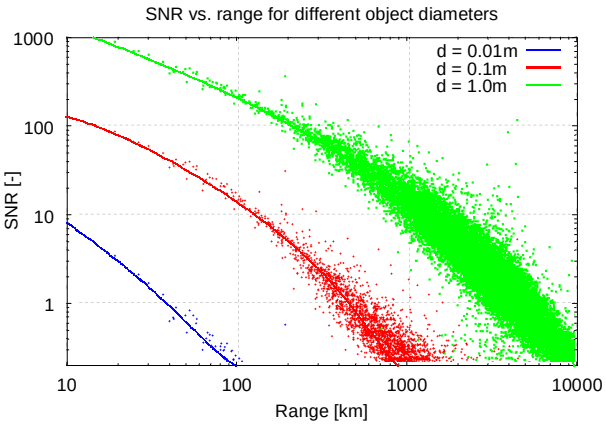

Fig. 1: Dependency of the SNR on detection range and object diameter (splines through PROOF results)

It can be seen that cm- and mm-sized objects only become visible within comparable short ranges below about 100km. The number of objects appearing in that range window is quite small, thus a large FOV would be favourable to increase the sample. However, there are technical constraints for the ratio of the focal length to the diameter of the aperture. In addition the resolution capabilities of the optical system and the sum of background signal per pixel increases with the FOV. Hence, a FOV of 30° seems to be a feasible and acceptable compromise and has been used for this work.

Besides the design criteria, the operational parameters have a significant impact on the SNR. Fig. 2 shows the influence of the integration time on the resulting SNR for a sensor on a SSO. The lower the range to the object gets, the higher is the angular velocity of the object.

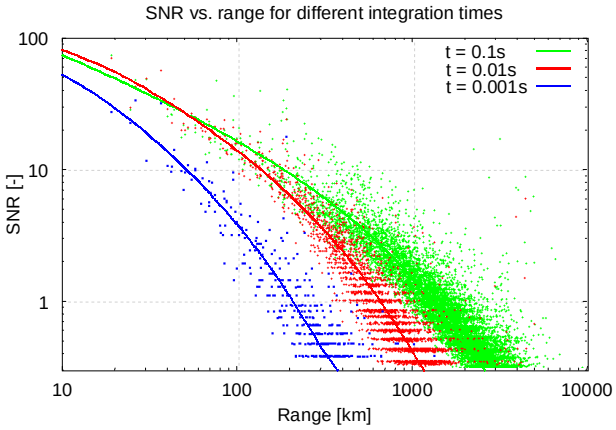

Fig. 2: Dependency of the SNR on the integration time for a 10cm object (splines through PROOF results)

The optimum choice for the integration time is a value close to the pixel dwell time. Here, as the passages of the objects are not orthogonal like for the ground-based case, the pixel dwell time is not constant for each passage. Long integration times increase the performance for more distance objects with respectively lower angular velocity. An integration time of 0.001s seems to be too short for all cases. For the detection of small objects, as we saw, a good performance in short distances is important. Here an integration time of 0.01s gives best results. The CCD matrix chosen for the following experiments is a 512x512 pixel matrix fitting very well to the integration time of 0.01s. Three orbits for the sensor have been analysed. The corresponding optimum configuration and the results to be expected are presented in the following.

3. SUN SYNCHRONOUS ORBIT

A sun synchronous orbit with 800km altitude will bring the sensor into the most dense region of the Earth's space debris environment. Usually, the mm-sized objects in that region are invisible to ground based instruments. This region is of high interest, as the high spatial densities of debris objects could provide a base for a setting in of collision cascading. The crossing rates as a function of the viewing direction are shown in Fig. 3. The object numbers are highest for viewing directions of –20° elevation (see also Fig. 4). For lower elevations the crossing rate is very small due to the appearance of the Earth in the FOV that covers most of the objects. For the azimuth, it can be seen that highest crossing rates can be expected from directions orthogonal to the plane of the sensor orbit. This is a consequence of the special angular distribution of the object flux. At the same time the line of sight orientation has an impact on the encounter duration and directionality.

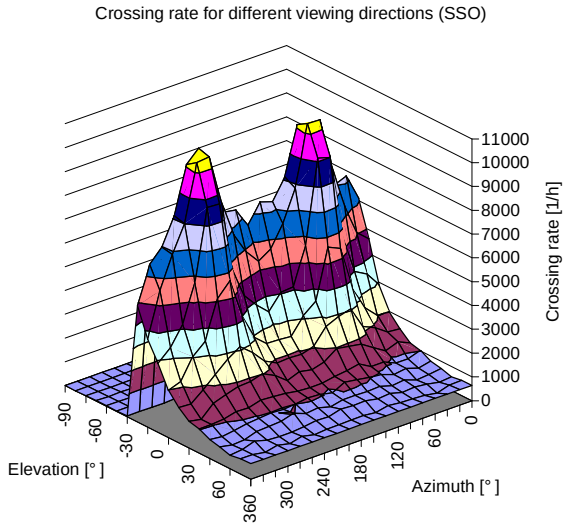

Fig. 3: Crossing rate in dependence of the viewing direction (SSO, all ranges, objects >5mm, FOV=1°)

The ranges of the objects approaching to the sensor can be estimated from Fig. 4. The high peak at an elevation of –20° appears at ranges that are too high to allow detections. High crossing rates within short ranges can be expected for an elevation of the LOS of 0°.

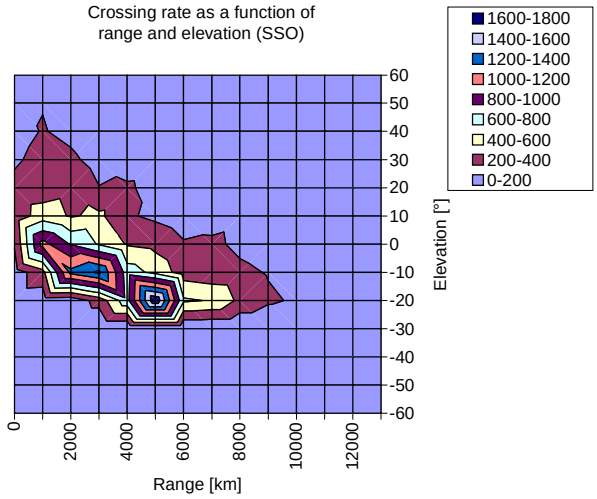

Fig. 4: Crossings per hour in dependence of range and elevation (SSO, objects >5mm, FOV=1°)

At the same time this elevation ensures a constant optimal illumination of the objects. For this, an earth oriented satellite with a viewing direction of 90° azimuth and 0° elevation away from the sun is chosen (see also [2]). Fig. 5 shows the detection rate per day in dependence of the detected diameters. The detection of about 10 objects below 1cm diameter per day can be expected. The brightness of the background during the experiment was at about 21 mag/arcsec². The smallest detectable objects are about 5mm in size.

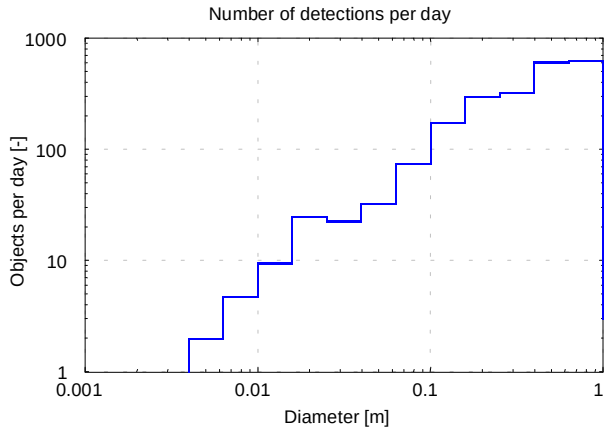

Fig. 5: Detections per day for SSO (result from 5 Monte Carlo runs)

This diameter threshold can be extended by using a narrower FOV. This, of course, would decrease the detection rate to a level that would be unacceptable from the statistical point of view. The presented configuration provides information in the desired diameter range with sufficient statistical relevance.

4. GEO TRANSFER ORBIT

This orbit is frequently used by several types of transfer vehicles. Moreover, there are only few demands from other types of mini-satellites for this kind of orbit, that could therefor become easily available for such a mission. A GTO spacecraft passes through all altitude regimes, with a particular high residence time in geostationary altitudes. For a sensor on a 0° inclination GTO, any object orbit should be visible, but the conditions for detection are deteriorated for some regions. While in the apogee the relative angular velocities to the GEO debris are quite low, angular velocities to the LEO objects in the perigee are very high. In addition the sampling time is short as the sensor only resides for about 1h per day in this altitude region.

To obtain constant optimal phase angles, a three axis stabilised platform with a viewing direction away from the Sun that must be adopted in dependence of the date would be favourable (sun-fixed). Like it is shown in Fig. 6 a right ascension of the LOS of 90° in the orbital plane provides best object illumination conditions for December 21. As Fig. 6 indicates, the orientation of the line of apsides with respect to the Sun influences the viewing geometry in relation to the sensor orbit. In addition to the annual rotation with respect to the Sun, this orbit, due to the low inclination, will be significantly influenced by the perturbation forces resulting from the non symmetric gravitational field. As a major consequence, the line of apsides will rotate with an inertial angular velocity of about 0.42° per day.

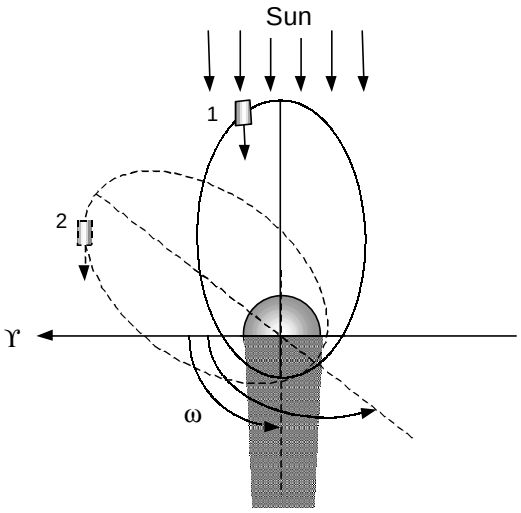

Fig. 6: Rotation of the sensor orbit causing a change in the relative viewing geometry (Dec. 21)

For each revolution a slightly deviating scenario and consequently different crossing and detection rates can thus be expected. Consequently, the impact of the Earth shadow on the observation result will also change. In addition, objects are invisible to the detector when the Earth is inside the FOV which is inevitable for 0° declination staring directions. It will thus be interesting to see how crossing rates of all objects and of invisible objects depend on the orientation of the line of apsides to the Sun (or: on the argument of perigee (ω) for Dec. 21). Fig. 7 shows the number of crossing objects > 1cm within a 2000km range window (i.e. the objects most likely to be detected) with respect to the attitude of the line of apsides (variation as indicated in Fig. 6).

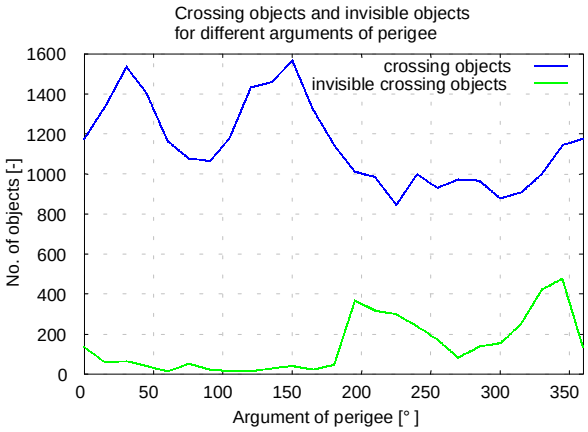

Fig. 7: number of all crossing and number of invisible objects per day for a variation of ω as indicated in Fig. 6 (range >2000km, objects >1cm)

It is quite remarkable that highest crossing rates occur at argument of perigees of 30° and 150°. This is mainly caused by the high number of LEO objects. The high numbers of invisible objects at the complementary angles are resulting from the same effect. The number of GEO objects encountered is more or less constant for all angles. Fig. 8 shows that the intersection area between the considered range band and the most populated area around 800km is much higher for the orbit with the perigee at 30° than for that with the perigee at 210°. In contrast to that, the intersection area inside the invisible band is higher for the orbit with the perigee at 210°. In addition to the intersection area, higher crossing rates can be expected from tangential intersection of the orbit than from radial ones which provide a shorter intersection length. The FOV cone on the orbit with 30° attitude mainly intersects the visible region in a radial way in contrast to the 210° orbit. High crossing rates at 90° and 180° do not occur due to similar reasons.

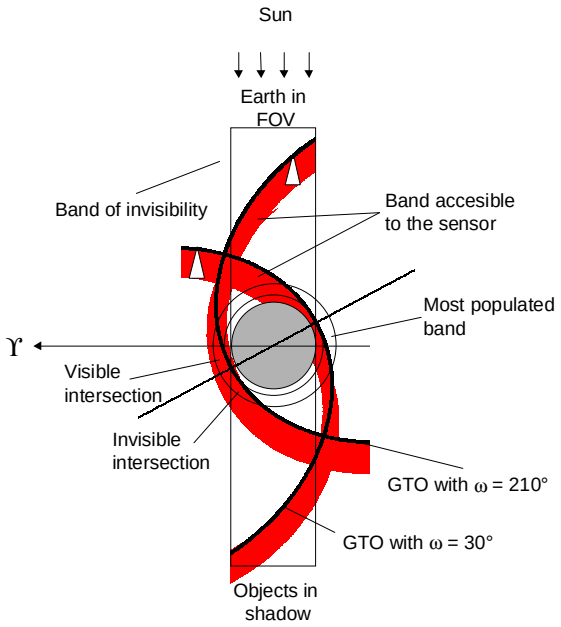

Fig. 8: Illustration of the intersection areas (GTO with ω = 30° and with ω = 210°)

For argument of perigees higher than 180° crossing rates remain on a low level as the sensor mainly stares towards the Earth during the perigee passage and outside the geostationary ring during the apogee passage. The results for two selected arguments of perigee (30° and 270°) combined with the viewing direction of 90° are shown in Fig. 9. The integration time chosen was 1s with a FOV of 30° and a 512x512 CCD matrix. Most of the detected objects between 1mm and 1m are LEO objects. As could be expected from Fig. 8, the detection rate for LEO objects for the 90° orbit is much lower than for the 30° orbit. During the perigee passages, the sensor is behind Earth encountering all objects in the dense region during their shadow passage by mainly radial orbit intersections. The number of GEO objects observed by a sensor on the orbit with 90° attitude is slightly higher. Satisfactory, also a considerable number of GTO objects can be detected.

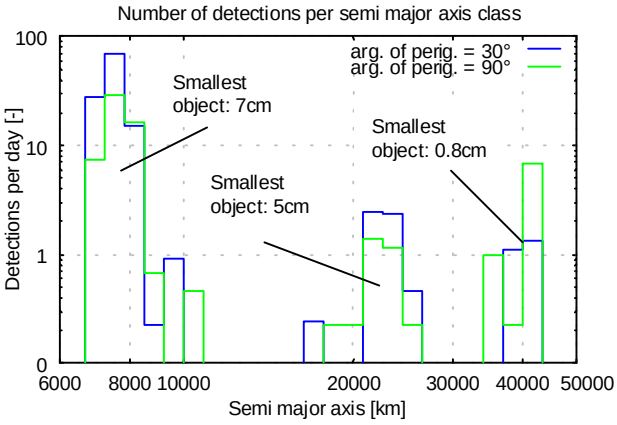

Fig. 9: Detections per day for GTO (Ω = 0°, ω = 30° and ω = 90°, right ascension of LOS = 90°, result from 5 Monte Carlo runs, objects between 1mm and 1m)

The lowest detected diameters reach from 7cm in LEO over 5cm in GTO to even 8mm in GEO. Due to the high angular velocity in the perigee, performance in the LEO region is deteriorated. Thus preference should be given to the observation of GTO and GEO objects. If the orbit can't be controlled, the initial orientation of the line of apsides with respect to the Sun should be chosen such that during its motion until the end of the mission the conditions are optimal for the observation of GTO and GEO objects (i.e. from 180° to 360°).

5. GEOSTATIONARY ORBIT

The geometric conditions for a sensor dedicated to the observation of GEO objects are comparably simple. Two scenarios have been analysed: A three axis stabilised platform providing a viewing direction constantly away from the Sun and an Earth oriented platform. For the sun-fixed viewing direction a geostationary sensor orbit has been selected. By this, geostationary objects can cross the sensors FOV for any orbital position. However, as the longitude of the sensor is fixed, new detections can only originate from objects drifting with respect to the platform. For the Earth oriented sensor a circular orbit 1000km below GEO (radius = 41164km) has been chosen. For half of the orbit revolution this sensor will encounter phase angles higher than 90°. For the other half of the revolution time the optical conditions should be good enough to allow several detections. Due to the distance of 1000km, more passages of geostationary and inclined geostationary objects will occur. The orbital period of the platform is at about 23h. Thus, within 24 day all regions of the

geostationary ring will have been observed. The distribution of the detected diameters for an integration time of 10s is shown in Fig. 10.

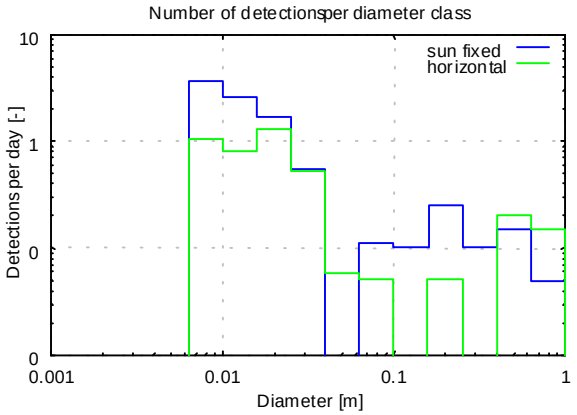

Fig. 10: Detections per day for a 3 axis stabilised and an Earth oriented sensor platform on GEO (result from 20 Monte Carlo runs)

The lowest detectable diameter is 8mm for both missions, where detection rates for the sun-fixed platform are higher due to the constant phase angle of 0°. GTO debris is contributing to the larger objects. Beside fragments, a high number of Solid Rocket Motor slag particles can be detected. The detection rates are high enough to provide a profound statistical base.

6. PERFORMANCE OF ORBITAL TELESCOPES

All sensor orbits analysed here are chosen such, that generally all inclination bands can be observed.

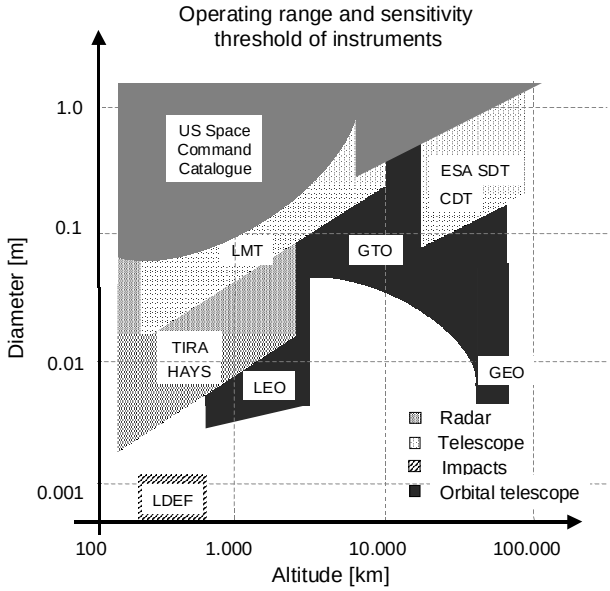

Fig. 11: Possible contribution of space based sensors to the current state of measurement results.

Fig. 11 summarises the results for the three orbits showing that space based telescopes can significantly improve our knowledge about the small size debris population. Using triangulation techniques and analysing the object's trace on the matrix will help to retrieve some of the orbital parameters of the objects.

7. CONCLUSIONS

Ground based optical and radar sensors can only provide an incomplete picture of the hazardous mm- and cm-sized particles in the Earth's space debris environment. ESA's PROOF'99 tool was used to simulate missions of small space based telescopes to detect objects in this size class in all altitudes. Three different configurations and scenarios were analysed focussing on different regions each. The selected orbits and the assumed instrument for this analysis are predestined for a pick-a-back launch on a mini satellite platform. A sensor on a SSO can detect a statistical relevant number of LEO objects, while sensors on GTO and GEO can provide information about cm-sized GTO and GEO objects. The results show that the observational gap (objects between 1mm and 1cm in LEO and objects between 1cm and 1m in all higher regions) can be covered to a satisfactory degree.

REFERENCES

1. Bendisch J., Krag H., Rosebrock J., Schildknecht T., Sdunnus H., Rex D., *Extension of ESA's MASTER Model to Predict Debris Detections*, Final report 12569/D/IM, Braunschweig, Germany, May 2000

2. Bendisch J., Hoffmann J. P., Liebscher R., Rollenhagen F., *Detection of Space Debris by the use of Space Based Optical Sensors*, Proceedings of the 1st European Conference on Space Debris, Darmstadt, Germany, April 1993

3. Lobb D. R., *Study on Optical Sensors for Space Debris Observation*, Final report, SIRA Research & Development, ESTEC Contract 9267/90/D/MD, November 1992

4. Alby F., Otrio G., Durin C., *Space Based Observations of Orbital Debris*, Conference paper IAA-00-IAA.6.4.04, 51st IAF congress, Rio de Janeiro, Brazil, October 2000